

**Figure 2.** (a) Transient difference spectra observed 30 ns and 1  $\mu$ s following photolysis of I. (b) Spectra of intermediates present 30 ns and 1  $\mu$ s after photolysis determined by adding the original pigment spectrum to the difference spectra above. The sample, regenerated ROS solubilized in 2% octyl  $\beta$ -D-glucopyranoside (octyl glucoside), was photolyzed with a 532-nm, 7-ns pulse from a frequency doubled Nd:YAG laser.

pigment is formed, the synthetic chromophore is not displaced from its binding site by 11-cis-retinal. Further, the hypothesis that the synthetic chromophore occupies the true pocket is supported by the fact that the pigment is stable in 1% ammonyx detergent which destroys metarhodopsin III formed from the native pigment.

To test the photochemical behavior of pigment I, we looked for photolysis intermediates using both low-temperature spectra and nanosecond laser photolysis. Low-temperature trapping studies were performed by standard procedures.<sup>12</sup> As shown in Figure 1, 436-nm illumination at  $-130$  °C yields a red-shifted absorption ( $\lambda_{\max} = 530$  nm), which is analogous to that due to the formation of batho in the case of native bovine rhodopsin.<sup>13</sup> Illumination at  $-85$  °C and subsequent warming to  $-55$  °C yield spectra with  $\lambda_{\max} = 495$  and 480 nm, respectively, and with slightly increased extinction. These spectral maxima are very close to those of the lumirhodopsin (lumi) and the metarhodopsin I stages of cattle rhodopsin.<sup>13</sup>

Laser photolysis studies were carried out as described previously,<sup>10</sup> except that  $90^\circ$  excitation was employed with path lengths through the sample of 2 mm for actinic light and 1 cm for the probe beam. Also, to maximize information obtained in the experiment with a minimum amount of material, spectra were obtained using multichannel detection. Figure 2 shows the transient difference spectra and the corrected spectra of the intermediates formed 30 ns and 1  $\mu$ s after photolysis, which for bovine rhodopsin represent the time scales of batho and lumi.<sup>10,14,15</sup> It is evident that the spectral changes observed in the case of I (with room temperature spectral maxima of batho and lumi intermediates at 560 and 470 nm) are very similar to those of native rhodopsin (560 and 475 nm, respectively<sup>10</sup>). Moreover, as shown in Figure 3, the kinetics of the decay of the 575-nm absorption are very similar to those seen in native rhodopsin.

(12) Yoshizawa, T. In *Photochemistry of Vision*; Dartnall, H. J. A., Ed.; Springer-Verlag: New York, 1972; pp 146-179.

(13) Yoshizawa, T.; Schichida, Y. In *Methods in Enzymology*; Packer, L., Ed.; Academic Press: New York, 1982; pp 333-354.

(14) Goldschmidt, Ch. R.; Ottolenghi, M.; Rosenfeld, T. *Nature (London)* **1976**, *236*, 169-173.

(15) We note that the 9-cis (isorhodopsin) isomer, which could be formed by illumination of batho in the case of the native pigment, cannot be present in the case of I. Thus, difference spectra of photolysis intermediates of I might be expected to differ slightly from those of native bovine rhodopsin. However, we worked under conditions in which isorhodopsin formation from bovine rhodopsin would be negligible.

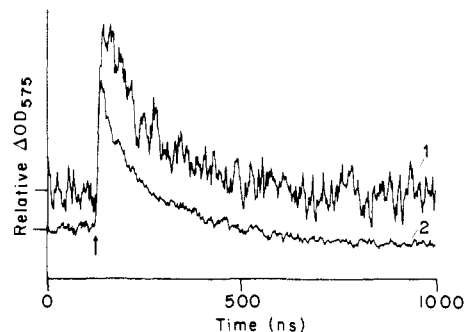


**Figure 3.** Decay kinetics following photolysis at room temperature of the 575-nm absorption in I (curve 1) compared with that in native rhodopsin (curve 2). Photolysis conditions were the same as those in Figure 2 with the photolysis pulse occurring at the time indicated by the arrow. The signal from I is noisier since it is small due to the low extinction of this pigment. The signal from native rhodopsin is scaled and offset for ease of comparison. The kinetics can be fitted by a single exponential decay of 135 ns.

The major conclusion of this work is that a visual pigment which has  $C_9=C_{10}$  and  $C_{10}-C_{11}$  bonds locked in their trans configurations produces photolysis intermediates which are very similar to those produced in native rhodopsin. This indicates that a significant rotation of the  $C_{10}-C_{11}$  bond is not an essential requirement for the bleaching sequence of rhodopsin to occur. The possibility that other bond rotations accompany  $C_{11}=C_{12}$  isomerization will be investigated in further studies.

**Acknowledgment.** This work was supported in part by a grant from the National Institutes of Health (EY 00983) to D.S.K. and by the Fund for Basic Research (administered by the Israeli Academy of Sciences and Humanities) to M.S. and by the Dutch Organization for Basic Research to W.D.G.

### Reorientation of the $CH_3$ Groups and Its High Activation Energy in $\sigma$ Radical Cations of Alkanes: ESR Observation for *n*-Butane<sup>+</sup>

Machio Iwasaki\* and Kazumi Toriyama\*

Government Industrial Research Institute  
Nagoya, Hirate, Kita, Nagoya 462, Japan  
Received April 28, 1986

In our first ESR observation of  $C_2H_6^+$  and other prototype alkane radical cations,<sup>1,2</sup> we have shown that the methyl group is rather rigid in the  $\sigma$  radical cations such as propane,<sup>+</sup> *n*-butane,<sup>+</sup> isobutane,<sup>+</sup> neopentane,<sup>+</sup> etc. This was somewhat surprising because of the deficiency of the C-C  $\sigma$ -bonding electrons, which might make the molecular framework somewhat more flexible. Information on the internal rotation of such one electron-loss species from the  $\sigma$ -bonding orbital must be of fundamental significance in chemistry. In the present work, we wish to report the hindering potential barrier for the  $CH_3$  reorientation in *n*-butane radical cations as the first example for such  $\sigma$  radical cations.

As is presented in our previous paper,<sup>2,3</sup>  $n-C_4H_{10}^+$  in  $CFCl_3$  or  $CFCl_2CF_2Cl$  exhibits the three-line spectrum with a coupling constant of 60.0 and 61.3 G, respectively, arising from the two in-plane end protons in the planar extended structure. Shortly later, Wang and Williams have shown that the spectrum of  $n-C_4H_{10}^+$  in  $CFCl_3$  gives resolvable substructure at 150 K and have obtained the coupling constant of 75.6 G,<sup>4</sup> which is considerably

(1) Iwasaki, M.; Toriyama, K.; Nunome, K. *J. Am. Chem. Soc.* **1981**, *103*, 3591.

(2) Toriyama, K.; Nunome, K.; Iwasaki, M. *J. Phys. Chem.* **1981**, *85*, 2149.

(3) Toriyama, K.; Nunome, K.; Iwasaki, M. *J. Chem. Phys.* **1982**, *77*, 5891.

(4) Wang, J. T.; Williams, F. *Chem. Phys. Lett.* **1981**, *82*, 177.

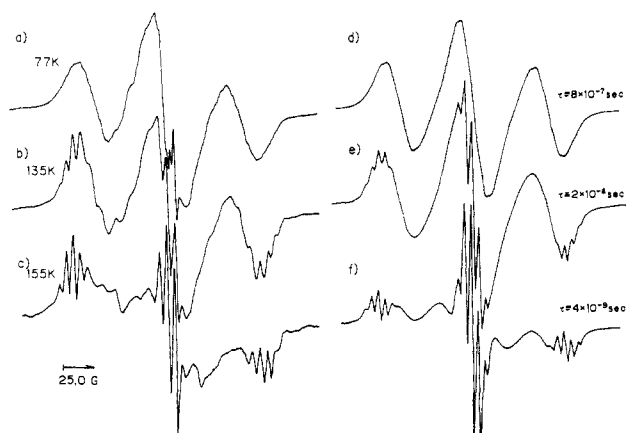


**Figure 1.** Temperature change of the ESR spectra of  $n\text{-C}_4\text{H}_{10}^+$  in  $\text{CFCl}_3$  (a-c) and those simulated by the modified Bloch treatment, assuming synchronized three-site jumping of the two methyl groups (d-f). The observation temperatures are (a) 77, (b) 135, and (c) 155 K. The lifetime ( $\tau$ ) and the line width assumed for the simulations are (d)  $8.0 \times 10^{-7}$  s, 7.0 G; (e)  $2.0 \times 10^{-8}$  s, 3.5 G; and (f)  $4.0 \times 10^{-9}$  s, 3.5 G, respectively. The hyperfine coupling constants assumed for the rigid state are  $a_1 = 60.0$  (2 H) and  $a_2 = 7.8$  G (4 H) for the methyl protons and  $a_3 = 5.5$  G (4 H) for the methylene protons.

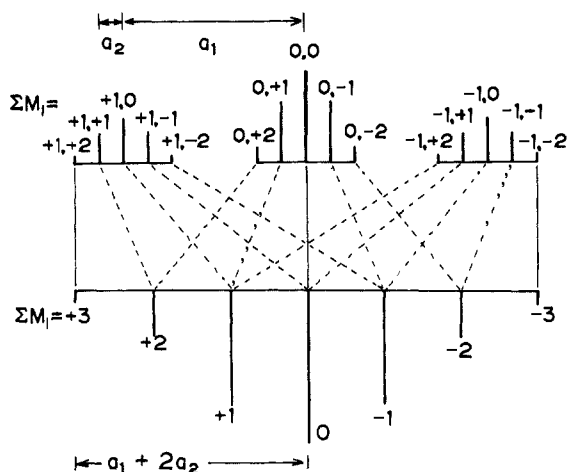


**Figure 2.** Illustration of the alternation of the line positions by reorientation of the methyl groups and the resulting line broadening of the spectra for the system with the two methyl groups having one large ( $a_1$ ) and two small ( $a_2$ ) sets of hyperfine coupling constants with the same sign.

higher than our value of 60.0 G at 77 K.<sup>2</sup> We had also observed this apparent temperature change of the spectral splittings in the very beginning of our studies. However, as shown in Figure 1, the peculiar line broadening of the main triplet spectrum indicates the involvement of some dynamical effect, suggesting that the center of the substructure might not give the true coupling constant for the main triplet. So, we did not give the separation of 75.6 G at  $\sim 150$  K as a coupling constant.<sup>2</sup>

Now we wish to present unescapable evidence for the reorientational motion of the  $\text{CH}_3$  groups giving the peculiar temperature change, based on the simulation by the modified Bloch treatment.<sup>5</sup> The reversible spectral change can be qualitatively interpreted by the following scheme: The main triplet with  $a_1 = 60.0$  G must split into five lines by the out-of-plane four protons ( $a_2$ ) in the two  $\text{CH}_3$  groups, and they further split into five lines by the four methylene protons ( $a_3$ ), although they are not well resolved at 77 K. Onset of the  $\text{CH}_3$  group reorientation results in the exchange of the methyl proton couplings. If one excludes the methylene proton coupling for a while, the outermost line position of the  $3 \times 5$  line spectrum must be invariant together with the central line, whereas the other lines must alter the line

**Table I.** Hyperfine Coupling Constants of  $n\text{-Butane}$  Radical Cations and Their Activation Energies and Frequency Factor for the Reorientation of the Methyl Group

matrices	$a(\text{CH}_3)$ , G		$a(\text{CH}_2)$ , G out-of-plane (4 H)	$E_a^b$ , kcal mol <sup>-1</sup>	$A,^b$ s <sup>-1</sup>
	in-plane (2 H)	out-of-plane (4 H)			
$\text{CFCl}_3$	+60.0	+7.8	(-)-5.5	2.4	$3.9 \times 10^{11}$
$n\text{-C}_4\text{F}_{10}$	+63.0	$\sim 0$	(-)-8.0	2.3	$1.8 \times 10^{11}$
INDO <sup>a</sup>	+68.0	-1.9	-4.9		

<sup>a</sup>Reference 2. <sup>b</sup>The activation energy and the frequency factor are obtained from the plot of  $\ln(\tau^{-1})$  vs.  $1/T$ .

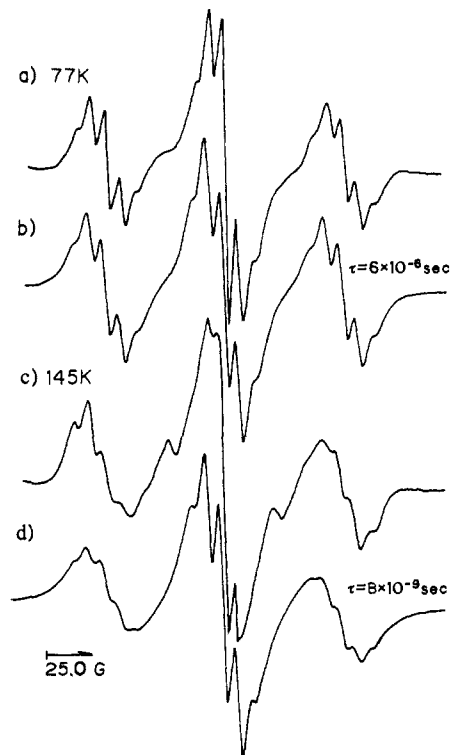


**Figure 3.** Temperature change of the ESR spectra of  $n\text{-C}_4\text{H}_{10}^+$  in  $n\text{-C}_4\text{F}_{10}$  and those simulated by the modified Bloch treatment, assuming the zero coupling for the four out-of-plane protons in the methyl groups ( $a_1 = 63.0$ ,  $a_2 = 0.0$  G) and  $a_3 = 8.0$  G for four methylene protons. The observation temperatures are (a) 77 and (c) 145 K. The lifetime ( $\tau$ ) and the line width assumed for the simulations are (b)  $6.0 \times 10^{-6}$  s, 7.0 G, and (d)  $8.0 \times 10^{-9}$  s, 5.5 G, respectively.

positions as is illustrated in Figure 2, provided that all the methyl proton coupling constants have the same sign. Therefore, the lines other than the outermost and the central lines must be broadened by the onset of the  $\text{CH}_3$  group reorientation. Thus, the well-resolved substructure due to the four methylene protons must appear on these three invariant lines with an increasing rate of the reorientation. It is clear that the coupling constant estimated from the center of the substructures on the invariant lines becomes larger than  $a_1$  by an amount of  $2a_2$ . So,  $a_2$  is estimated to be  $(75.6 - 60)/2 = 7.8$  G. The simulated spectral changes using  $a_1 = 60.0$ ,  $a_2 = 7.8$ , and  $a_3 = 5.5$  G (Table I) reproduce the fine detail of the observed spectra at various temperatures as shown in Figure 1.

The activation energy, 2.4 kcal/mol, suggests that the potential barrier is not very much reduced from 2.8 kcal/mol for ethane<sup>6</sup> by loss of one of the  $\sigma$ -bonding electrons. Since a similar temperature change of the spectra is reported for  $n\text{-C}_4\text{H}_{10}^+$  in  $\text{CF}_3\text{-CCl}_3$ ,<sup>7</sup> the coupling constants as well as the activation energy may be similar in this matrix. On the other hand, a marked tem-

(6) Pitzer, K. S. *Discuss. Faraday Soc.* **1951**, 10, 66.

(7) (a) Tabata, M.; Lund, A. *Radiat. Phys. Chem.* **1984**, 23, 545. (b) Lindgren, M.; Lund, A.; Dolivo, G. *Chem. Phys.* **1985**, 99, 103. (c) Lund, A.; Lindgren, M.; Dolivo, G.; Tabata, M. *Radiat. Phys. Chem.* **1985**, 26, 591.

(5) Miyagawa, I.; Itoh, K. *J. Chem. Phys.* **1962**, 36, 2157.

perature change in the outermost line positions was not observed in  $n\text{-C}_4\text{F}_{10}$  at 77–160 K, while the five-line substructure is clearly seen even at 77 K<sup>3</sup> as shown in Figure 3. This may suggest that  $a_2$  is essentially zero in this matrix. In such a case, marked line narrowing of the main triplet ( $a_1 = 63.0$  G) by the  $\text{CH}_3$  reorientation cannot be expected as is easily understood from the illustration in Figure 2. Therefore, the five-line substructure with  $a_3 = 8$  G must be due to the four protons in the methylene group, as is assigned in our previous work.<sup>3</sup> The simulated spectra along this line nicely reproduce the observed temperature change giving

essentially the same activation energy as shown in Figure 3 and in Table I. The temperature change in  $\text{CFCl}_2\text{CF}_2\text{Cl}$  also suggests that the activation energy is similar to that in  $\text{CFCl}_3$ . Thus, it is concluded that the planar extended structure is maintained throughout the observation temperatures in all the matrices and the small variation of the coupling constant from matrix to matrix is ascribable to the interaction with matrix.

The interpretation in terms of a slight nonplanarity by Lund and his co-workers<sup>7</sup> should be reconsidered in the light of the present study.

## Book Reviews

**Comprehensive Chemical Kinetics. Volume 25: Diffusion-limited Reactions.** By Stephen A. Rice (Shell Research B. V., Rijswijk, The Netherlands). Elsevier Science Publishers: Amsterdam and New York. 1985. xiv + 404 pp. \$132.25. ISBN 0-444-42354-0.

This book consists of a critical review of theoretical treatments of diffusion-limited reactions. In the first half of the book, these are compared with experimental data. First is discussed the basic theory of diffusion-limited reactions (Smoluchowski etc.) and limitations of same (Chapter 2). Modifications include coulombic effects (ion/ion reactions), long-range transfer effects (dipole/dipole interactions, exchange interaction, and electron tunnelling), and rotational diffusion (Chapters 3–5). Chapters 6 and 7 treat the escape or recombination of reactants formed in pairs, both uncharged (atom/atom and radical/radical) and charged (ion/ion). The last five chapters are devoted to theory, which is interpreted with lucid commentary, comprising a critique of the diffusion equation and molecular-pair treatments, refinements to include many-body effects, the variational principle, phenomenological Brownian motion, and the kinetic theory of fluids.

This is a research monograph addressed to the specialist and will, I suspect, be most appreciated by experimenters trying to keep abreast of theory. The book, unlike previous volumes in this series, is written by a single author. It is well organized and clearly written, and the author has definite opinions to express. Data from radiation chemistry are cited extensively; thus coulombic effects are discussed with use of data on hydrated and solvated electrons; and there is a section on ions formed in spurs.

Any book on this subject will be dense. Here some 550 references are cited in 400 pages. Despite a full Table of Contents, the author's hard work is rendered inexcusably inaccessible to the reader by the absence of an author index and by an inadequate subject index, compiled by another hand.

Michael Henchman, *Brandeis University*

**Advances in Polymer Science. Volume 75. Epoxy Resins and Composites II.** Edited by K. Dusek (Institute of Macromolecular Chemistry, Czechoslovak Academy of Sciences). Springer-Verlag: Berlin, Heidelberg, New York, Tokyo. 1986. viii + 180 pp. \$45.00. ISBN-3-540-15825-1, hardcover; ISBN-0-387-15825-1, softcover.

This volume contains four readable and informative critical reviews on aspects of epoxy resins and composites, a subject of great technological importance. It is well edited and produced. Each article provides good perspective on its subject and offers examples of recent research.

In *The Interphase in Epoxy Composites*, L. T. Drzal demonstrates that the heterogeneous region near the surfaces of both the matrix and the reinforcing fiber strongly affects the properties of epoxy composites, often deleteriously. Advances in composite performance may depend on better understanding and control of this interphase region.

In *Epoxy Adhesion to Metals*, R. G. Schmidt and J. P. Bell emphasize the importance of adhesion under wet conditions. Substantially improved structural adhesives and corrosion-resistant coatings will become possible if ways are found to improve wet adhesion. The authors recommend a search for better chemical coupling agents and better metal pretreatments.

Application of FT-IR and NMR to Epoxy Resins, by E. Mertz and J. L. Konig, includes a lucid introduction to FT-IR and NMR and examples of how they have been used to characterize epoxy resins, curing processes, and properties of cured materials. The authors point out the advantages of diffuse reflectance and photoacoustic FT-IR techniques for studies of surfaces.

In *Kinetics, Thermodynamics and Mechanism of Reactions of Epoxy Oligomers with Amines*, B. A. Rozenberg details the complexities of catalysis, autocatalysis, autoinhibition, and side reactions that affect the properties of amine-cured epoxy resins. Information gained from model compound studies is analyzed, and a useful discussion of kinetics during the critical late stages of crosslinking is provided.

The editor plans a four-volume series that will contain 21 reviews by authorities on epoxy materials. The high quality of the present volume indicates that the series will be a valuable resource for those interested in the field.

Frank N. Jones, *North Dakota State University*

**Fluidization.** Edited by J. F. Davidson (Cambridge University), R. Clift (University of Surrey), and D. Harrison (University of Exeter). Academic Press Inc.: London. 1985. xiv + 733 pp. \$96.50. ISBN 0-12-205552-7.

Fluidized beds are an important tool of the chemical industry and find wide use as reactors in petroleum and metallurgical processing, for syntheses and polymerizations, for gasification and liquefaction of solid fuels, and in many other areas. However, this book does not deal with the how and why of any of this. Instead, it deals with the research efforts going on at present aimed at understanding the basic physics of this form of gas/solid contacting. If you want to know what researchers are doing in this area and what they have found, this is your book.

As with the first edition published 15 years ago, this volume consists of contributions by researchers into various aspects of fluidization. The 21 chapters (29 contributing authors) fall into three groups. First, there are eleven chapters dealing directly with the physical aspects of the normal dense-phase fluidized bed (bubbles and slugs, distributors and jetting, self-mixing and mixing of different solids, hydrodynamic theory and stability, heat transfer and influence of internals, and so on). Six chapters deal with related phenomena (spouted, high-velocity and large-particle fluidized beds, flow of solids through pipes and valves, elutriation, and gas/liquid/solid fluidization). The remaining four chapters of this volume deal with aspects of particular applications (drying of solids, growth and coating of particles, modeling of solid-catalyzed gas-phase reactions, coal combustion).

In recent years there has been an enormous outpouring of reports and technical papers on fluidization, many appearing only in obscure proceedings of limited circulation, or as preprints of oral presentations. Just the thought of keeping abreast of all this literature is depressing. Hence, this volume is welcome in that it aims to bring all these findings together. There are over 1600 references and numerous tables listing the reported data and correlations. This is a handsome and carefully edited volume which should be invaluable to researchers in the basics of fluidization.

Octave Levenspiel, *Oregon State University*

**Superacids.** By G. A. Olah and G. K. Surya Prakash (University of Southern California) and J. Sommer (Louis Pasteur University). John Wiley & Sons: New York. 1985. xv + 371 pp. \$57.95. ISBN 0-471-88469-3.

This book is a survey of superacids and their chemistry and represents the culmination of several review articles by the principal author. The book is essentially divided into three parts. The first part details the various superacid systems available. These include liquid Brønsted acids, Lewis acids, and solid superacids and lists relative acidities of these systems in terms of the  $H_0$  acidity function. The second and most extensive portion of the book deals with carbocation structures. The whole range of classical trivalent "carbenium" ions to pentacoordinate non-